

Influence of photon angular momentum on ultrafast demagnetization in nickel

F. Dalla Longa,* J. T. Kohlhepp, W. J. M. de Jonge, and B. Koopmans

Department of Applied Physics and Center for NanoMaterials, Eindhoven University of Technology, P.O. Box 513,
5600 MB Eindhoven, The Netherlands

(Received 27 September 2006; revised manuscript received 10 January 2007; published 28 June 2007)

The role of pump helicity in laser-induced demagnetization of nickel thin films is investigated by means of pump-probe time-resolved magneto-optical Kerr effect in the polar geometry. Although the data display a strong dependency on pump helicity during pump-probe temporal overlap, this is shown to be of nonmagnetic origin and not to affect the demagnetization. By accurately fitting the demagnetization curves, we show that demagnetization time τ_M and electron-phonon equilibration time τ_E are not affected by pump helicity. Thereby, our results exclude direct transfer of angular momentum to be relevant for the demagnetization process and prove that the photon contribution to demagnetization is less than 0.01%.

DOI: [10.1103/PhysRevB.75.224431](https://doi.org/10.1103/PhysRevB.75.224431)

PACS number(s): 75.40.Gb, 75.70.Ak, 78.20.Ls, 78.47.+p

Since the observation by Beaurepaire *et al.* that excitation by femtosecond laser pulses can induce a demagnetization in a nickel thin film on a subpicosecond time scale,¹ laser-induced magnetization dynamics received a growing attention.²⁻⁸ The possibility of optically manipulating spins on such an ultrafast time scale offers, indeed, many potential applications in technology. Beside the technological relevance, research in this field is motivated by scientific interest, the microscopic mechanisms that lead to ultrafast magnetization response being not yet fully understood.

Recently, we presented a microscopic model that successfully explains the demagnetization process in terms of phonon- or impurity-mediated Elliot-Yafet-type electron-electron spin-flip scattering, phonons and impurities providing the required transfer of angular momentum to the spins.⁹ In the model, possible “nonthermal” contributions to the demagnetization, like angular momentum transfer from laser photons or enhanced spin-flip scattering during pump-probe overlap, are disregarded since the total number of photons involved in the process is estimated to be too small to give rise to sizable effects.⁴ Using a complementary approach, Zhang and Hübner (ZH) attempted to explain the demagnetization process as the result of the combined action of spin orbit coupling (SOC) and the interaction between spins and laser photons.¹⁰ The authors disregard the role of phonons, motivated by the expectation that conventional scattering mechanisms lead to spin-lattice relaxation times of some tens of picoseconds, too slow to account for the observed ultrafast demagnetization.

Searching for a unified picture of laser-induced demagnetization, it is important to understand which processes play a major role in different materials. Recently, it has been found, for instance, that nonthermal processes are dominating in garnets.¹¹ In those experiments, circularly polarized pump pulses generate a coherent magnetic field (inverse Faraday effect) that applies a torque on the magnetization vector. On the other hand, it has been known for some years that pump polarization does not have a major influence in the spin response to laser excitation in transition metals.¹²⁻¹⁵ However, this qualitative observation has never been supported by a quantitative and systematic study, leaving several fundamental questions open: To what extent does pump polarization influence the demagnetization? Are the time scales of the

process affected by pump polarization? Can different handedness of pump circular polarization induce a magnetization precession of opposite phases like in Ref. 11? It is the aim of this paper to provide such a systematic study. Our analysis shows that the demagnetization time τ_M and electron-phonon equilibration time τ_E are independent of pump polarization. This provides quantitative support to some of the approximations used in Ref. 9 and suggests that the mechanisms described by ZH might not be appropriate to describe ultrafast demagnetization in nickel.

The sample under investigation consists of a 10 nm thick Ni film sputtered on a SiO substrate and capped with 2 nm of copper to prevent from oxidation. The thickness of the ferromagnet has been especially chosen to match the light penetration depth (~ 15 nm for Ni at a wavelength of 785 nm) in order to uniformly heat up the film throughout its thickness. Pump and probe pulses have a temporal full width at half maximum of 70 fs and are focused onto the same 8 μm diameter spot on the sample through a high aperture laser objective, with a final fluence of 2 and 0.1 mJ/cm^2 , respectively. The laser pulses hit the sample at almost normal incidence: in this polar geometry, the probe pulses are mostly sensitive to the out of plane component of the magnetization, M_z . A 2 kG field applied perpendicular to the film surface leads to a canted magnetization state inducing a finite M_z , as depicted in Fig. 1 (inset).

We make use of two distinct experimental techniques: time-resolved magneto-optical Kerr effect (TR-MOKE) and time-resolved magnetization modulation spectroscopy (TIMMS). In the TR-MOKE setup, a quarter wave plate enables the tuning of pump helicity between right circularly polarized (RCP) and left circularly polarized (LCP), and intermediate states. The linearly polarized probe pulses pass through a photoelastic modulator (PEM) before being focused onto the sample; the PEM modulates the polarization of the pulses from right circular to left circular with a frequency f_{PEM} . After reflection off the sample, the pulses are sent to a photodetector through another polarizer crossed with the first; it can be shown⁴ that in these conditions, the $2f_{\text{PEM}}$ component of the detected signal is proportional to the laser-induced changes of the Kerr rotation, $\Delta\theta$. In the TIMMS setup, one modulates the helicity of the pump pulses with a PEM while probe pulses are linearly polarized; there-

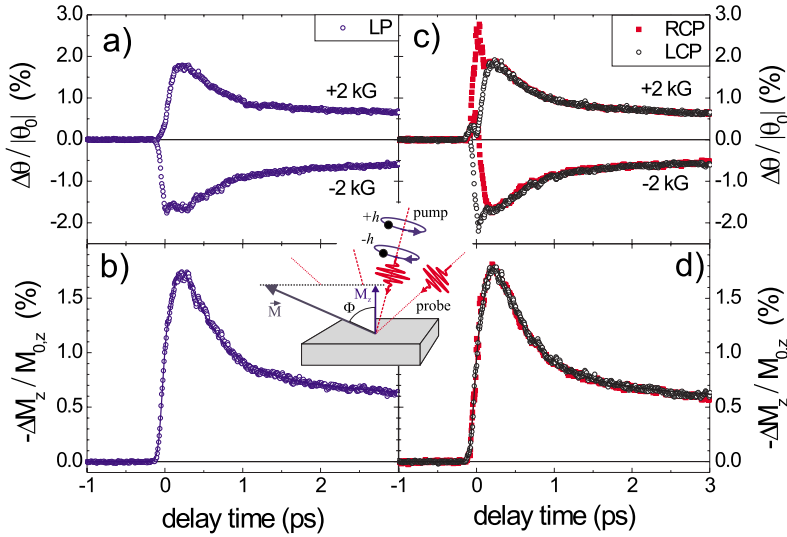


FIG. 1. (Color online) Typical TR-MOKE response to (a) linearly polarized (LP) light pumping and (c) right (open circles) and left (full squares) circularly polarized (CP) light pumping, for an out of plane applied field of ± 2 kG. (b) Genuine magnetization response to LP pumping obtained by averaging the curves in (a). (d) Genuine magnetization response to right (open circles) and left (full squares) CP pumping obtained by averaging the corresponding right and left CP curves in (c). The solid lines in (b) and (d) are fits to the data using Eq. (1). Inset: Schematic representation of the experiment; the canted magnetization forms an angle Φ with the normal to the surface; CP pump photons carry a whole quantum of angular momentum $\pm\hbar$; probe pulses are sensitive to M_z .

fore, the differences between the responses to RCP and LCP pumping are directly detected. It can be shown¹⁶ that the $1f_{PEM}$ component of the detected signal is proportional to $\Delta\theta$. In conclusion, with the TR-MOKE experiments, we set the pump polarization and measure the induced time-dependent demagnetization; with the TIMMS experiments, we modulate the pump polarization and measure the time-dependent differences between the demagnetization induced by RCP pumping and LCP pumping.

Before presenting the results, let us briefly explain the idea behind our experiment. Considering that the macroscopic magnetization is given by the space average of the atomic magnetic moments $\vec{\mu} = \mu_B(\vec{L}_e + g\vec{S}_e)$, where μ_B is the Bohr magneton, \vec{L}_e and \vec{S}_e are the orbital and spin part of electron momentum, respectively, and $g \approx 2$ for nickel, it is clear that the observed demagnetization is due to a momentum transfer from the electrons to “somewhere else.” The allowed demagnetization channels are given by conservation of total angular momentum $\vec{J} = \vec{L}_e + \vec{S}_e + \vec{L}_{latt} + \vec{L}_{ph}$, where \vec{L}_{latt} and \vec{L}_{ph} represent the angular momentum carried by the phonons and the photons involved in the process, respectively. Note that a Stoner excitation as well as a magnon can, in principle, induce a change in \vec{S} . On the contrary, the process in which a Stoner excitation occurs by emitting and/or absorbing a magnon conserves the total spin momentum and thereby does not contribute to the demagnetization.

More generally, demagnetization can happen due to (i) exchange between orbital and spin part of electrons’ momentum, (ii) momentum transfer from electrons to the lattice, and (iii) a similar transfer to the laser field. Note that all three mechanisms require SOC. In addition to (iii), the role of the laser field can be different than direct angular momentum transfer. First, (a) the laser field could lead to an increased efficiency of mechanisms (i) and (ii), due to, e.g., enhanced SOC in the excited state. On itself, however, the laser field does not participate as source of angular momentum in this scenario. Second, (b) via the inverse Faraday effect, a coherent magnetization (parallel to the wave vector) is generated in the excited state. Such a coherent magnetization can be

probed itself,¹⁴ as will be discussed later in this paper. However, in this scenario, the magnitude of the magnetization vector is left behind unchanged after coherent effects are over. Alternatively, (c) the coherent magnetization can act a torque on the ground state magnetization vector, triggering a precession thereof without affecting the length of the magnetization vector. An example of this can be found in Ref. 11. In our polar configuration, however, the initial displacement would be parallel to the film plane and thereby not observable during the first picosecond.¹⁷ In the context of the foregoing analysis, it is our aim to show *quantitatively* that direct momentum transfer to the laser field (iii) is an insignificant process. This will be investigated using circularly polarized pump pulses: Since CP photons carry a whole quantum of angular momentum $\pm\hbar$ along (RCP) or opposite to (LCP) the direction of light propagation, transfer of angular momentum should induce a demagnetization *only* when photon helicity and magnetization are antiparallel, while the magnetization should actually increase when they are parallel. Having realized that neither of the alternative scenarios in which the laser field is involved [(a)–(c)] affects the angular momentum balance in a direct way, the insignificance of mechanism (iii) would imply that the key of ultrafast demagnetization is in an ultrafast momentum exchange within the electron and lattice system.

Our experimental configuration, in which \vec{M} is only partially canted out of the sample plane, could seem inconvenient with respect to using a sample with perpendicular anisotropy. However, our approach has the advantage that we can investigate the influence of pump helicity not only on demagnetization effects (i.e., affecting the modulus of \vec{M}) but also on orientational effects (i.e., affecting the canting angle Φ). This is particularly interesting in view of the already mentioned results in Ref. 11, where pump polarization is found to trigger a precessional motion of the magnetization vector in a garnet film. On a longer (hundreds of picoseconds) time scale, a precessional motion could be observed in our measurements; however, no dependence of the precession on the pump polarization was found.

Let us now focus on our TR-MOKE experiments. The

result of a standard experiment, i.e., using linearly polarized light pumping, is presented in Fig. 1(a), where the transient Kerr rotation normalized to its static value, $\Delta\theta/|\theta_0|$, is plotted. When an out of plane field of 2 kG is applied, the Kerr rotation displays a maximum at ~ 250 fs after laser excitation; if we reverse the field, we see that the same qualitative response with opposite sign is obtained. The genuine magnetic response, $\Delta M_z/M_{0,z}$ (where $M_{0,z}$ represents the static value of M_z), is proportional to $\Delta\theta^+ - \Delta\theta^-$, the difference between the two Kerr rotation transients corresponding to opposite field directions, i.e., we are taking into account only the part of the signal that changes sign upon magnetization reversal; this is shown in Fig. 1(b).

The final data set can be fitted with a function that describes the demagnetization process in terms of energy redistribution among electrons, phonons, and spins upon laser excitation, using the phenomenological three-temperature model.¹ We derived an analytical solution in the limit of low laser fluence, neglecting spin specific heat and assuming an instantaneous rise of the electron temperature upon laser excitation.¹⁸

$$-\frac{\Delta M_z(t)}{M_{0,z}} = \left\{ \left[A_1 F(\tau_0, t) - \frac{(A_2 \tau_E - A_1 \tau_M) e^{-t/\tau_M}}{\tau_E - \tau_M} - \frac{\tau_E (A_1 - A_2) e^{-t/\tau_E}}{\tau_E - \tau_M} \right] \Theta(t) + A_3 \delta(t) \right\} \star \Gamma(t), \quad (1)$$

where $\Gamma(t)$ is the Gaussian laser pulse, \star represents the convolution product, $\Theta(t)$ is the step function, and $\delta(t)$ is the Dirac delta function. The constant A_1 represents the value of $-\Delta M_z/M_{0,z}$ after equilibrium between electrons, spins, and lattice is restored. Cooling by heat diffusion is described by the function $F(\tau_0, t)$. In our case, the data are well described by an inverse square root like behavior, i.e., $F(\tau_0, t) = (\sqrt{t/\tau_0} + 1)^{-1}$, with $\tau_0 \gg \tau_E, \tau_M$. The constant A_2 is proportional to the initial electron temperature rise. The constant A_3 represents the magnitude of state filling effects during pump-probe temporal overlap that can be well described by a delta function. The most important parameters are τ_E and τ_M ; the former describes the time scale of electron-phonon (e-p) interaction (typically ~ 450 fs) that equilibrates the electron with the phonon system; the latter describes the time scale of the magnetization loss (typically ~ 100 fs). It can be shown¹⁸ that both electron- and phonon-induced contributions can be incorporated into a single parameter τ_M , which makes (1) ideally suited to extract a characteristic time scale without any presumptions about the underlying mechanisms. For the data of Fig. 1(b), we obtained $\tau_M = 73$ fs (Ref. 19) and $\tau_E = 440$ fs.

In Fig. 1(c), the demagnetization following RCP and LCP light pumping is presented. As already reported in Refs. 14 and 15, when the system is pumped with CP light, an additional peak appears at 0 ps delay, superimposed to the usual response. The extra peak does not change sign upon magnetization reversal, while it changes sign when pump helicity is inverted. The origin of the peak lies in the so called specular inverse Faraday effect (SIFE) and specular optical Kerr ef-

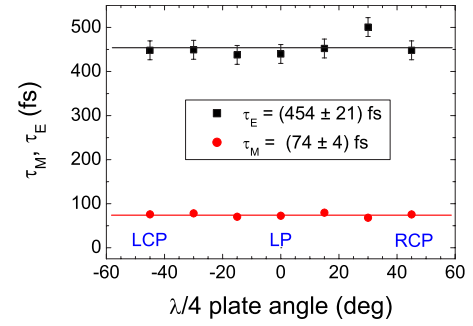


FIG. 2. (Color online) Demagnetization time τ_M (circles) and electron-phonon equilibration time τ_E (squares) against the orientation of the $\lambda/4$ plate: the values are nicely scattered around averages of 74 and 454 fs, respectively (solid lines), showing no dependency on pump helicity. The error bars (not visible for the circles) are the standard deviations.

fect (SOKE) contribution: in a simplified picture, CP photons transfer their angular momentum to the electronic orbits and the enhanced orbital momentum is then sensed by the probe beam. These coherent third order effects are not the main concern of this paper; the interested reader is referred to, e.g., Refs. 11, 14, 15, and 20. Besides the presence of the additional peak, we notice that a demagnetization is *always* observed, independent of pump helicity, even when photons angular momentum and magnetization are parallel. This shows that neither direct transfer of angular momentum between laser field and spins nor a helicity dependence of laser-enhanced spin-flip scattering is the main mechanism giving rise to the demagnetization process. As to the latter, and in the spirit of the ZH model, we cannot exclude a helicity-independent laser-mediated angular momentum transfer within the electronic system. However, when neglecting the phonon system, such a mechanism will leave the demagnetized material in a highly excited state and, for $g \approx 2$ and the ground state magnetism dominated by spin momentum, cannot lead to quenching of M by more than 50%.

Finally, we quantitatively explore whether the presence of the extra peak in Fig. 1(c) (related to the pump helicity) influences (i) the time scale τ_M of ultrafast demagnetization or (ii) details of the final (demagnetized) state, a few hundred femtosecond after laser excitation.

To address point (i), we proceed as in the linear case by subtracting the two signals obtained at opposite fields: as it can be seen in Fig. 1(d), the two curves overlap showing no evident difference. In order to carry out a quantitative analysis, we repeated the procedure for different values of pump helicity and fitted the resulting curves with Eq. (1). The obtained values of τ_M and τ_E are plotted as function of pump helicity in Fig. 2: the data are nicely scattered around average values $\bar{\tau}_M = 74 \pm 4$ fs and $\bar{\tau}_E = 454 \pm 21$ fs and show no measurable dependency on pump helicity. This unambiguously provides a quantitative proof that the time scales of demagnetization and e-p equilibration are completely independent of pump polarization.

As for point (ii), absorption of a circularly polarized photon leads to coherent transfer of angular momentum to the orbital component of the excited electronic state. Our data

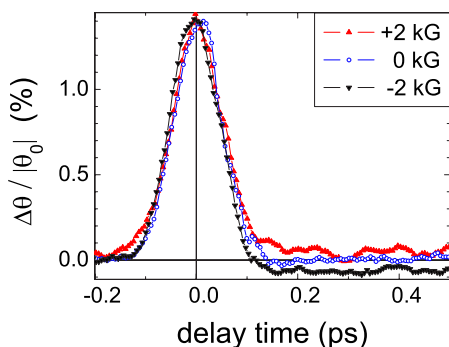


FIG. 3. (Color online) TIMMS measurements: the field-dependent signal after the SIFE/SOKE peak is due to a correlation between pump helicity and intensity (lines are guides to the eyes).

show, however, that after dephasing and reestablishing of the ground state ratio of spin and orbital momentum in the magnetic state, no significant transfer to the electronic system (magnetic moment) is left. As we argued before in Ref. 4, this small transfer is expected to be of the order of $\frac{\Delta M_{\text{phot}}}{M_0} \sim \pm 0.01\%$. In order to detect such a subtle contribution, a TIMMS modulation scheme can be adopted. A typical data set obtained from TIMMS measurements is plotted in Fig. 3, the different curves corresponding to different applied field values. The peak around 0 ps delay is once again the SIFE/SOKE contribution, and it is independent of the applied field as one would expect from the TR-MOKE experiments. After the SIFE/SOKE peak, the signal goes back to zero if no field is applied, while stabilizing to a small, though finite, value of

$\pm 0.05\%$ when an out of plane field of ± 2 kG is applied. If this subtle contribution came from a genuine difference in response to RCP and LCP pumping due to a change in ΔM_z or Φ induced by direct transfer of angular momentum, one would expect it not to change sign upon field reversal. Therefore, we conjecture that this small contribution is actually due to a finite correlation between pump helicity and pump intensity, due to the not exactly perpendicular incidence and to the presence of mirrors between the PEM and the sample. Therefore, the TIMMS measurements confirm the estimate of a photon contribution of the order of $\pm 0.01\%$ at most.

In conclusion, we investigated the ultrafast spin dynamic response to CP laser light excitation in a Ni thin (10 nm) film by means of TR-MOKE and TIMMS, aiming at a quantitative estimate of the influence of pump helicity on laser-induced demagnetization. The analysis of the data showed that the typical time scales involved in a demagnetization experiment are not affected by the polarization of the pump pulse; in particular, we determined a demagnetization time $\tau_M = 74 \pm 4$ fs and an e-p equilibration time $\tau_E = 454 \pm 21$ fs. Moreover, the high resolution TIMMS measurements support the picture of a photon contribution to the demagnetization process in nickel of not more than $\pm 0.01\%$. This provides a quantitative justification to some of the approximations used in Ref. 9.

The authors acknowledge W. Hübner for fruitful discussions. The work is supported in part by the European Communities Human Potential Programme under Contract No. HRPN-CT-2002-00318 ULTRASWITCH.

*f.dalla.longa@tue.nl

- ¹E. Beaupaire, J. C. Merle, A. Daunois, and J. Y. Bigot, *Phys. Rev. Lett.* **76**, 4250 (1996).
- ²J. Hohlfeld, E. Matthias, R. Knorren, and K. H. Bennemann, *Phys. Rev. Lett.* **78**, 4861 (1997).
- ³A. Scholl, L. Baumgarten, R. Jacquemin, and W. Eberhardt, *Phys. Rev. Lett.* **79**, 5146 (1997).
- ⁴B. Koopmans, M. van Kampen, J. T. Kohlhepp, and W. J. M. de Jonge, *Phys. Rev. Lett.* **85**, 844 (2000).
- ⁵H. Regensburger, R. Vollmer, and J. Kirschner, *Phys. Rev. B* **61**, 14716 (2000).
- ⁶L. Guidoni, E. Beaupaire, and J.-Y. Bigot, *Phys. Rev. Lett.* **89**, 017401 (2002).
- ⁷E. Beaupaire, G. M. Turner, S. M. Harrel, M. C. Beard, J. Y. Bigot, and C. A. Schmuttenmaer, *Appl. Phys. Lett.* **84**, 3465 (2004).
- ⁸M. Vomir, L. H. F. Andrade, L. Guidoni, E. Beaupaire, and J. Y. Bigot, *Phys. Rev. Lett.* **94**, 237601 (2005).
- ⁹B. Koopmans, J. J. M. Ruigrok, F. Dalla Longa, and W. J. M. de Jonge, *Phys. Rev. Lett.* **95**, 267207 (2005).
- ¹⁰G. P. Zhang and W. Hübner, *Phys. Rev. Lett.* **85**, 3025 (1999).
- ¹¹F. Hansteen, A. Kimel, A. Kirilyuk, and T. Rasing, *Phys. Rev. Lett.* **95**, 047402 (2005).

- ¹²G. Ju, A. Vertikov, A. V. Nurmikko, C. Canady, G. Xiao, R. F. C. Farrow, and A. Cebollada, *Phys. Rev. B* **57**, R700 (1998).
- ¹³E. Beaupaire, M. Maret, V. Haltè, J.-C. Merle, A. Daunois, and J.-Y. Bigot, *Phys. Rev. B* **58**, 12134 (1998).
- ¹⁴R. Wilks, R. J. Hicken, M. Ali, B. J. Hickey, J. D. R. Buchanan, A. T. G. Pym, and B. K. Tanner, *J. Appl. Phys.* **95**, 7441 (2004).
- ¹⁵R. Wilks, N. D. Hughes, and R. J. Hicken, *J. Phys.: Condens. Matter* **15**, 5129 (2003).
- ¹⁶B. Koopmans, J. E. M. Haverkort, and W. J. M. de Jonge, *J. Appl. Phys.* **85**, 6763 (1999).
- ¹⁷Note that coherent magnetization could also induce a permanent change in the magnetization. However, such an effect is identical to the direct transfer mechanism (iii).
- ¹⁸Derived in a straightforward way by analytically solving the set of differential equations that describe the heat flow; details to be published elsewhere.
- ¹⁹We would like to remark that the same data set would yield $\tau_M = 135$ fs if empirically fitted by $(1 - e^{-t/\tau_m})\Delta T_e(t)$ as used in other works instead of Eq. (1).
- ²⁰P. J. Bennett, V. Albanis, Yu. P. Svirko, and N. I. Zheludev, *Opt. Lett.* **24**, 1373 (1999).